

Hydrophobic Surface Treatment of Carbon Black Nanoparticles in Isopropyl Alcohol Solution Using He/SF₆ Atmospheric Plasma Jet

Mu Kyeom Mun¹, Lee Won Ho¹, Jin Woo Park¹, Doo San Kim¹,
Geun Young Yeom^{1,2,*}, and Dong Woo Kim^{1,*}

¹*School of Advanced Materials Science and Engineering, Sungkyunkwan University, Suwon, Kyunggi-do, 16419, South Korea*
²*SKKU Advanced Institute of Nanotechnology (SAINT), Sungkyunkwan University, Suwon, Kyunggi-do 16419, South Korea*

Nanoparticles in a solution can be modified by various methods including wet treatment, UV light treatment, and plasma treatment for the functionalization of the nanoparticles. Especially, for the plasma treatment of nanoparticles in a solution, hydrophilic treatment is generally carried out by forming –OH in the solution while the plasma treatment system is located at the outside of the nanoparticle solution. In this study, using a He/SF₆ atmospheric plasma jet (APPJ) sources located outside and inserted in the IPA solution with carbon black nanoparticles, carbon black nanoparticles were modified to improve hydrophobic properties. By inserting the plasma jet tip in the solution, the carbon black nanoparticles were more easily modified compared the plasma jet located outside of the solution. After the He/SF₆ plasma treatment of carbon black nanoparticles with the APPJ in the solution, the contact angle of the sprayed-coated carbon black was increased from ~30 to ~140° while no significant change of contact angle was observed for the carbon black nanoparticles treated by the APPJ located outside of the solution. After the He/SF₆ plasma treatment, fluorine percentage of ~7.97% in the carbon black was observed without noticeable thickness change of carbon black nanoparticles. It is believed that, the fluorine radicals dissolved in the solution form C–F_x bonding on the carbon black surface and increase the hydrophobicity significantly. This technique can be applied in modifying the surface properties of various other particles in solution.

Keywords: Nanoparticle, Surface Treatment, Plasma Jet, Carbon Black, Hydrophobic.

1. INTRODUCTION

Nanoparticles are applied to various industries such as bio, environment, energy, etc. and, for the application of the nanoparticles, many researchers have investigated modification methods of the nanoparticles by using dry treatment, wet treatment, UV light treatment, etc.^{1–8} In the case of dry treatment such as plasma treatments, only the area exposed to the plasma is treated, and, to be used in a vacuum system, a nanoparticle collector need to be installed.⁹

For wet treatment and UV light treatment, it is known that the treatment time is generally long due to the slow reaction rates even though the nanoparticles are uniformly treated in the solution.^{4,5}

Atmospheric pressure plasma jet (APPJ) was also applied to improve the reaction of the nanoparticles in the

solution by forming active species on the surface of the solution containing the nanoparticles through the irradiation of the plasma on the surface.^{10,11} The reactive species formed on the surface of the solution diffuse into the solution and modify the nanoparticles. One of the drawbacks of this method is that the nanoparticles are modified only by the reactive species diffused in the solution. Therefore, to increase the reactive species in the solution and to improve the modification of the nanoparticles, the APPJ units inserted in the solution were investigated.^{12,13} Even though the modification of the nanoparticles was improved by inserting the APPJ in the solution due to the increased reaction of the plasma with the solution, due to the use of process gases such as Ar, He, O₂, H₂, and air in the solvents with –OH functional groups, only the effects of OH radicals formed in the solution were observed.^{14–18} The nanoparticle solvent with the –OH functional groups

*Authors to whom correspondence should be addressed.

irradiated by the plasma generates OH radicals and the nanoparticles exposed to OH radicals are modified to have hydrophilic properties.^{19–22}

Therefore, until now, most of the researches on the modification of nanoparticles in the solution using the APPJ treatment have been concentrated in changing the properties of nanoparticles to more hydrophilic in the solvent with the –OH functional groups.^{23–34} The solvents such as perfluorooctanoic acid, perfluorooctane sulfonate, etc. contain F atoms and tend to modify materials surface to be hydrophobic when they are dissociated by plasmas.^{35–37} In this study, for the hydrophobic treatment of the nanoparticles in a solution, not for the hydrophilic properties, the APPJ was inserted in an isopropyl alcohol (IPA) mixed with carbon black nanoparticles and the plasma was generated in the solution with a He/SF₆ gas mixture.

As an application to hydrophobic treatment of carbon black nanoparticles in an IPA, styrene-butadiene rubber (SBR), which is used for automobile tire thread, was fabricated.^{38,39} The tire thread requires lower rolling resistance for fuel efficiency and higher wet traction for stability, and for the lower rolling resistance and higher wet traction, carbon black is generally blended in SBR.^{40–49} Also, it is known that the use of hydrophobic treated

carbon black in SBR tends to increase the wet traction and decrease rolling resistance by preventing the wetting of SBR surface.^{50–55} Therefore, in this study, carbon black nanoparticles in an IPA was treated hydrophobically by using the He/SF₆ plasma generated with an APPJ inserted in (and outside of) the solution and the effect of plasma conditions on the hydrophobic properties of carbon black nanoparticles were investigated.

2. EXPERIMENTAL DETAILS

2.1. APPJ Module Design

The APPJ module used in this experiment is shown in Figure 1(a) for separate parts of the jet module, (b) for cross-section of the jet module, and (c) for the assembled jet. The jet module was a double-cone shape jet composed of top and bottom electrodes made of aluminum and a Teflon separator between the two electrodes. At the bottom cone tip, 1.5 mm diameter hole was formed for the emission of the jet discharge.

The top and bottom cone shaped electrodes were thermal spray-coated with 400 μm thick anodized aluminum to operate as dielectric barrier discharge (DBD) and to prevent arcing on the electrode surface. The distance between the two electrodes were kept at 1 mm. 60 kHz AC power

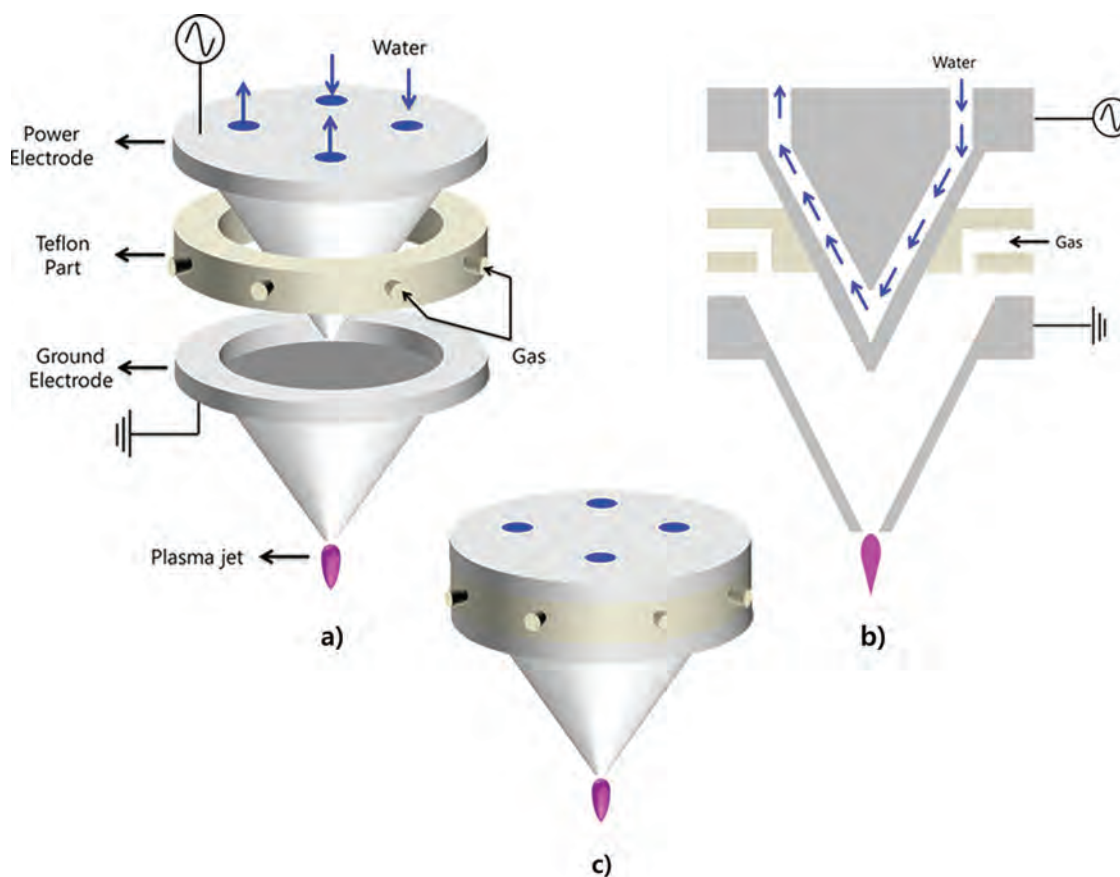


Figure 1. The APPJ module used in this experiment. (a) Disassembled figure of APPJ module, (b) cross-sectional figure of the APPJ module, and (c) assembled figure of APPJ module.

was connected to the water-cooled top power electrode and the bottom electrode was grounded. Discharge gas was connected to the Teflon separator. DBD was formed between the two electrodes, and the plasma was emitted at the tip of the bottom grounded cone.

2.2. Carbon Black Treatment

1 g of ~50 nm diameter carbon black nanoparticles (Graphene Supermarket) was mixed in a beaker with 500 ml IPA and dispersed by a sonicator for 90 min to form a carbon black solution.

The carbon black solution in the beaker was treated with the APPJ with the configurations shown in Figure 2(a) outside of the solution and (b) in the solution. When the APPJ was inserted in the solution with the configuration in Figure 2(b), to prevent spillover of the solution, a latex was covered on the beaker and a gas outlet hole was formed to prevent the increase of pressure in the beaker. As the process gas, He(2 slm)/SF₆ (0.5 slm) was used and the 60 kHz AC voltage was applied to the top power electrode to form a plasma. Figure 3 shows the images of the plasmas formed by the APPJ for different operating voltages of (a) 2.1 kV, (b) 2.7 kV, and (c) 3.3 kV. For the treatment of the carbon black nanoparticles, 3.3 kV of AC voltage was used in the experiment. Also, to investigate the differences in the surface characteristics of carbon black nanoparticles treated with the methods shown in Figures 2(a) and (b), the plasma treated carbon black nanoparticles were coated

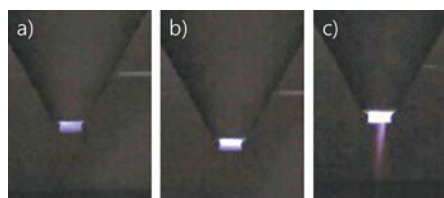


Figure 3. Images of the plasmas formed by the APPJ for different operating voltages of (a) 2.1 kV, (b) 2.7 kV, and (c) 3.3 kV. For the treatment of the carbon black nanoparticles, 3.3 kV of AC voltage was used in the experiment.

on polyimide substrates using a spray gun and the water contact angle was measured.

2.3. Styrene-Butadiene Rubber Polymerization

To fabricate SBR, which is used for automobile tire tread, butadiene (sigma-aldrich, 434787) and styrene (sigma-aldrich, S4972) were mixed with the ratio of 3:1.⁵⁸ 0 g, 0.05 g, 0.1 g, and 0.15 g of as-is carbon black nanoparticles and hydrophobic plasma treated carbon black nanoparticles obtained using the method in Figure 2(b) were mixed with the 10 cc of SBR solution and the mixed solutions were sonicated for 5 minutes for the dispersion of carbon black nanoparticles in the SBR solution. For the polymerization of the SBR solution mixed with carbon black nanoparticles, *N*-Butyllithium (sigma-aldrich, 230707) was added to the SBR solution with the ratio of 10:3.^{58,59} The polymerization was taken for 20 min and

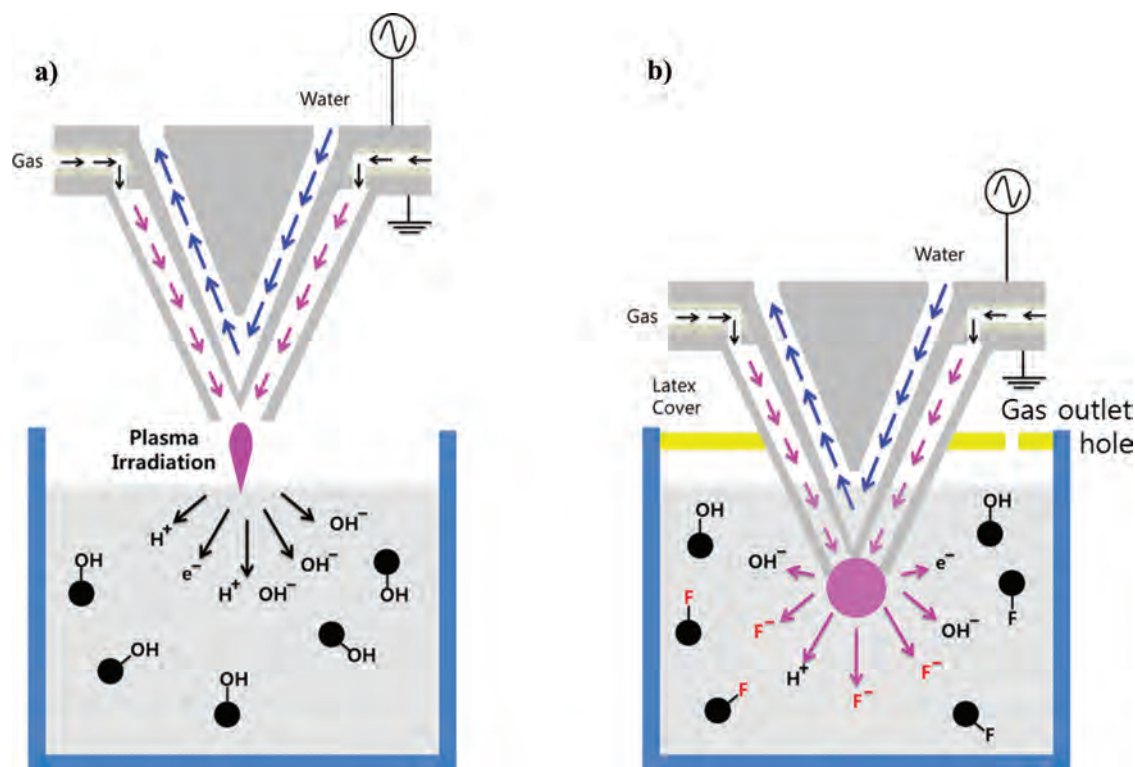


Figure 2. Carbon black solution in the beaker treated with the APPJ with the configurations (a) outside of the solution and (b) in the solution.

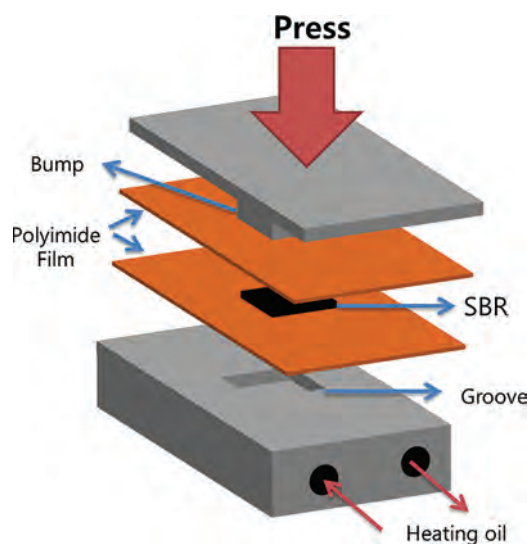


Figure 4. Hot pressing method used in the experiment to fabricate SBR film with carbon black nanoparticles with/without He/SF₆ plasma treatment and, for easier loading and removal of the SBR film during the hot pressing, polyimide films were inserted as shown in the figure.

the polymerized SBR was collected and pressurized for 5 minutes at 100 °C to obtain a SBR film. For the SBR film, the collected polymerized SBR was pressurized with the pressure of 1 kg/cm² for one min, followed by the pressurization with 0.5 kg/cm² for 4 min. Figure 4 shows the hot pressing method used in the experiment and, for easier loading and removal of the SBR film during the hot pressing, polyimide films were inserted as shown in Figure 4. The fabricated SBR film with the carbon black nanoparticles was dried in a dry oven for 50 minutes at 150 °C.

2.4. Analysis and Measurements

Contact angles on the carbon black spray coated on polyimide substrates and on fabricated SBR film mixed with different carbon black nanoparticles were measured using a contact angle analyzer (SEO, phoenix 450). Scanning electron microscope (FE-SEM, HITACHI, S-4700) was used to observe the morphology change of carbon black nanoparticles. The change of surface composition of the carbon black nanoparticles before and after the plasma treatment was investigated using X-ray photoelectron spectroscopy (XPS, thermo VG SIGMA PROBE).

3. RESULTS AND DISCUSSION

3.1. Carbon Black Contact Angle

Contact angles of carbon black nanoparticles coated on the polyimide substrates after the plasma treatment using the methods in Figures 2(a) and (b), that is, out-of-solution and in-solution, respectively, were measured as a function of plasma treatment time and the results are shown in Figure 5.

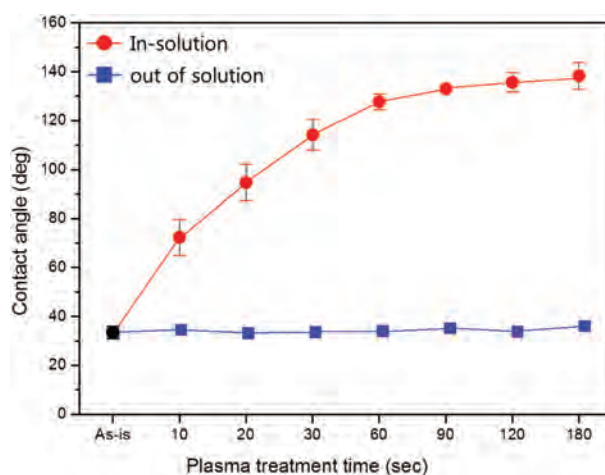


Figure 5. Contact angles of carbon nanoparticles coated on the polyimide substrates after the plasma treatment with the APPJ located out-of-solution and in-solution, measured as a function of plasma treatment time.

As the plasma treatment gas, He(2 slm)/SF₆ (0.5 slm) was used and the 3.3 kV 60 kHz AC voltage was applied to the top power electrode. As shown in Figure 5, the contact angle of untreated carbon black nanoparticle was ~33° and, the increase of plasma treatment time up to 180 s did not change the contact angle significantly for the carbon black treated with configuration in Figure 2(a). However, for the carbon black treated with the configuration in Figure 2(b), the contact angle increased significantly up to ~140° with increasing the plasma treatment time to 180 s. When the APPJ is located outside of the carbon black nanoparticle solution, the plasma is difficult to react with the solution, therefore, it generally takes very long time (from tens of minutes to a few hours) for the plasma treatment and tends to modify the material surface hydrophilically by forming OH radicals as investigated by other researchers.²³⁻³⁴ However, when the APPJ is located in the solution, due to more direct reaction of plasma with the solution, the modification of the carbon black nanoparticles was much faster than the plasma treatment at the outside of the solution.

Figures 6(a) and (b) show the carbon black nanoparticle solutions in a beaker treated with the configuration in Figure 2(b) just after the treatment and after 1 day storage after the treatment, respectively.

The carbon black nanoparticle solutions were treated for different plasma treatment time. The carbon black nanoparticles having hydrophilic properties are well dispersed in the IPA solution, therefore, no separation of carbon black nanoparticles with IPA was observed until the carbon black nanoparticles were treated by the plasma less than 60 s. However, when the plasma treatment time is longer than 60 s, the carbon black nanoparticles are separated from IPA after 1 day of storage because the carbon black nanoparticles are modified hydrophobically enough as shown in Figure 6(b) after 60 s.

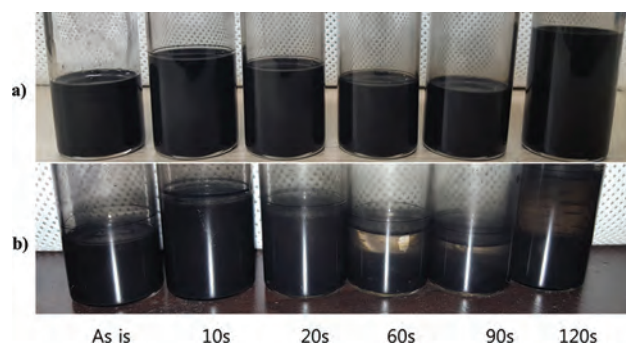


Figure 6. Carbon black nanoparticle solutions in a beaker treated with the configuration in Figure 2(b). (a) Just after the treatment and (b) after 1 day of treatment. When the plasma treatment time is longer than 60 s, the carbon black nanoparticles are separated from the IPA after 1 day of storage because the carbon black nanoparticles are modified hydrophobically.

3.2. Carbon Black Chemical Composition

The chemical composition and binding states of the carbon black nanoparticles in the IPA solution after the plasma treatment was investigated with XPS and the results are shown in Table I and Figure 7 for (a) fluorine and (b) carbon.

As the plasma treatment condition, the conditions in Figure 6 with the APPJ in the solution were used. As shown in Table I, the as-is carbon black is mostly composed of carbon except for a small percentage of carbon on the surface. However, as the surface of the carbon black is modified with the He/SF₆ plasma in the solution, due to the dissociation of SF₆ in addition to the dissociation of IPA by the plasma, atomic percentages of fluorine and oxygen were increased up to 7.97% and 9.78%, respectively. In Figures 7(a) and (b), the results on XPS narrow scan data of fluorine and carbon are shown, respectively. In the case of fluorine peak, with increasing the plasma treatment time, the formation and increase of the peak intensity related to C–F bonding was observed at ~685.5 eV and, an additional peak possibly related to C–F₂ bonding was observed at ~689 eV when the plasma treatment time further increased to 360 s. In the case of carbon peaks, as shown in Figure 7(b), the increase of plasma treatment time increased the bonding peaks related to C–O/C–CF at ~286 eV and C–F_x at ~288.5 eV indicating the formation of C–O bonding and increased C–F_x bonding with

Table I. Chemical composition of the carbon black nanoparticles in an IPA solution before and after the plasma treatment investigated with XPS.

Treatment time	F	C	O
Plasma treated			
360 s	7.97	82.25	9.78
180 s	2.29	89.11	8.59
90 s	1.26	94.02	4.72
As-is			
0 s	–	96.4	3.6

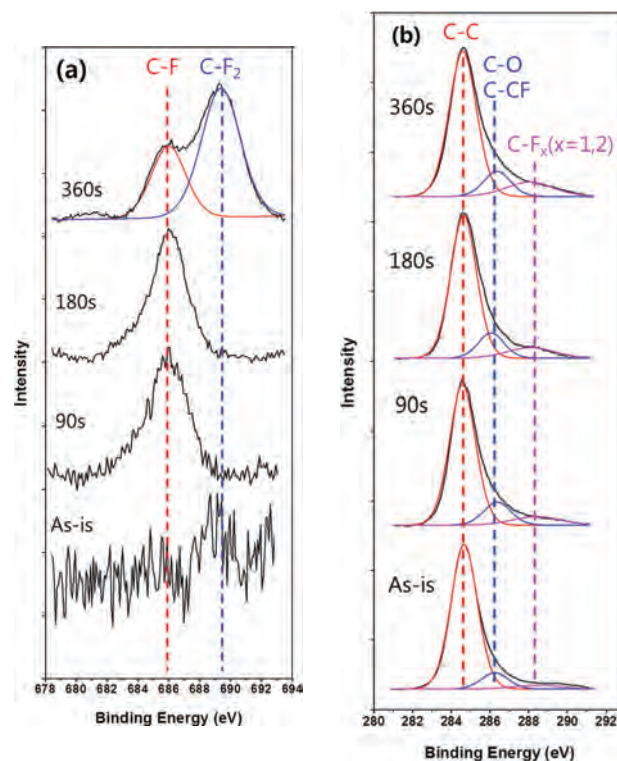


Figure 7. XPS narrow scan data of (a) fluorine and (b) carbon of the carbon black nanoparticles in the IPA solution after the plasma treatment with the APPJ in the solution.

increasing the plasma treatment time.^{60,61} Therefore, from Table I and Figure 7, it is found that the surface of carbon black nanoparticles is modified with fluorine dissociated from SF₆ in addition to OH radical formed in the solution, and which makes the carbon black surface hydrophobic even with –OH on the surface.

3.3. Carbon Black SEM Image

The morphologies of carbon blacks before and after the plasma treatment were observed using SEM and the results are shown in Figures 8(a) and (b) for as-is and after the plasma treatment with the APPJ in the solution, respectively. The carbon black was treated with the plasma with the condition of Figure 7 for 360 sec. The carbon black solution were dried for SEM observation before and after the plasma treatment. As shown in the figures, the size of the carbon black particles before the plasma treatment was ~50 nm and, after the plasma treatment, no significant change in size was observed indicating no noticeable etching or deposition of carbon black nanoparticles by fluorine on the surface of carbon black. Therefore, by the plasma treatment, only the surface of the carbon black nanoparticles was modified.

3.4. SBR Contact Angle

One of the applications of the hydrophobically treated carbon black nanoparticles is the SBR for tire. As shown in

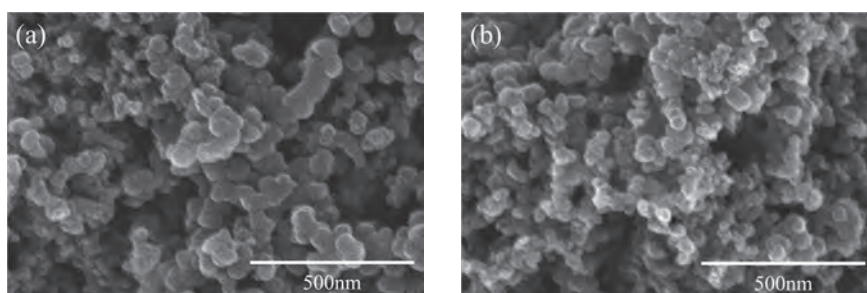


Figure 8. Morphologies of carbon blacks observed by SEM before and after the plasma treatment with the APPJ in the solution: (a) Is for as-is and (b) is after the plasma treatment.

the experimental section, 0 g, 0.05 g, 0.1 g, and 0.15 g of as-is and plasma treated carbon black nanoparticles with the APPJ in the solution were blended with the 10 cc of SBR solution and the SBR films were formed by pressurizing the SBR after the polymerization of the SBR solutions blended with carbon black nanoparticles. Figure 9 shows the contact angles of the pressurized SBR films measured as a function of carbon black weight in the SBR solution for as-is and plasma treated carbon black nanoparticles. As shown in the figure, the SBR mixed with carbon black nanoparticles exhibited higher contact angle, however, the contact angle was not significantly dependent on the concentration of carbon black nanoparticles.

If the contact angles of SBR with the carbon black nanoparticles with/without plasma treatment are compared, the contact angle of SBR with as-is carbon black nanoparticles was $\sim 60^\circ$ while that of SBR with the plasma treated carbon black particles was increased to $\sim 97^\circ$, therefore, more hydrophobic property of SBR with the plasma treated SBR could be obtained. The tire thread formed with the hydrophobic SBR is known to have enhanced wet traction by preventing hydroplaning and enhanced fuel efficiency due to low rolling resistance as mentioned earlier. Therefore, it is believed that, the

enhance properties of tire can be obtained through the hydrophobic plasma treatment of the carbon black mixed with SBR.

4. CONCLUSION

In this study, carbon black nanoparticles in an IPA were treated hydrophobically by using a He/SF₆ plasma generated with APPJs located outside of solution and in the solution and the effects of He/SF₆ plasma on the properties of carbon black nanoparticles were investigated. The surface of carbon black was significantly modified by the He/SF₆ plasma generated with the APPJ in the solution by showing the change of contact angle from 33° to 140° after 3 min. of plasma treatment while no significant change of the carbon black surface was observed for the plasma generated with the APPJ located out of the solution. When the carbon black nanoparticles were blended in SBR, which is used for the tire thread, the increase of contact angle of SBR surface from $\sim 60^\circ$ to $\sim 97^\circ$ was observed by using the carbon black nanoparticles treated with the APPJ in the solution, which enhances the properties of tire such as enhanced wet traction, improved fuel efficiency, etc. The hydrophobic properties of carbon black nanoparticles treated with the He/SF₆ plasma in the IPA solution was related to the fluorination of the carbon black surface by the modification of carbon black nanoparticle surface without changing the morphology of the particles.

Acknowledgment: This study was supported by the NRF-2016M3A7B4910429. This work was carried out through a project supported by Research Fellow (NRF-2016R1A6A3A11935139).

References and Notes

1. Q. Shi, N. Vitichuli, J. Nowak, J. M. Caldwell, F. Breidt, M. Bourham, X. Zhang, and M. McCord, *Eur. Polym. J.* 47, 7 (2011).
2. S. Hosseini, S. Madaeni, A. Khodabakhshi, and A. Zendeenam, *J. Membr. Sci.* 365, 1 (2010).
3. H. Xiong, *J. Mater. Chem.* 20, 21 (2010).
4. J. Zhao, M. Milanova, M. M. Warmoeskerken, and V. Dutschk, *Colloids Surf. Physicochem. Eng. Aspects* 413 (2012).
5. T. W. Woolerton, S. Sheard, E. Reisner, E. Pierce, S. W. Ragsdale, and F. A. Armstrong, *J. Am. Chem. Soc.* 132, 7 (2010).

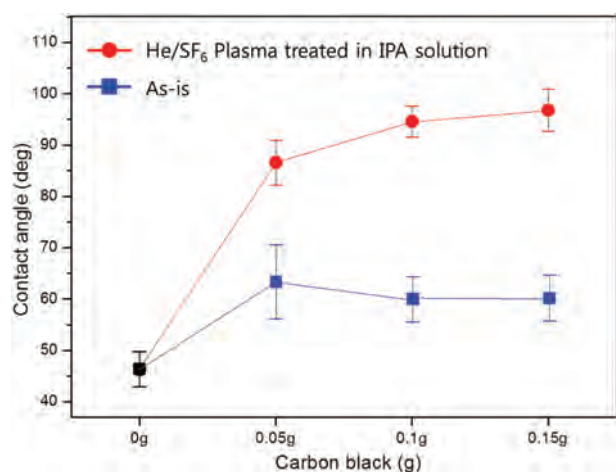


Figure 9. Contact angles of the pressurized SBR films measured as a function of carbon black concentration in SBR for as-is and plasma treated carbon black nanoparticles.

6. H. Huang and L. Tang, *Energy Convers. Manage.* 50, 3 (2009).
7. H. Wang, R. Cote, G. Faubert, D. Guay, and J. Dodelet, *The Journal of Physical Chemistry B* 103, 12 (1999).
8. C. Moreno-Castilla, M. Lopez-Ramon, and F. Carrasco-Marin, *Carbon* 38, 14 (2000).
9. R. Kumar, P. Cheang, and K. Khor, *J. Mater. Process. Technol.* 113, 1 (2001).
10. C. Van Gils, S. Hofmann, B. Boekema, R. Brandenburg, and P. Bruggeman, *J. Phys. D* 46, 17 (2013).
11. T. Takamatsu, K. Uehara, Y. Sasaki, H. Miyahara, Y. Matsumura, A. Iwasawa, N. Ito, T. Azuma, M. Kohno, and A. Okino, *RSC Advances* 4, 75 (2014).
12. G. Saito and T. Akiyama, *Journal of Nanomaterials* 16, 1 (2015).
13. J. Kang, O. L. Li, and N. Saito, *Nanoscale* 5, 15 (2013).
14. B. Sun, M. Sato, and J. S. Clements, *J. Electrostatics* 39, 3 (1997).
15. T. Ishijima, H. Hotta, H. Sugai, and M. Sato, *Appl. Phys. Lett.* 91, 12 (2007).
16. P. Bruggeman, T. Verreycken, M. A. Gonzalez, J. L. Walsh, M. G. Kong, C. Leys, and D. C. Schram, *J. Phys. D* 43, 12 (2010).
17. D. Mariotti, J. Patel, V. Švrček, and P. Maguire, *Plasma Processes and Polymers* 9, 11 (2012).
18. K. Kitano, H. Aoki, and S. Hamaguchi, *Japanese Journal of Applied Physics* 45, 10S (2006).
19. Y. H. Kim, Y. J. Hong, K. Y. Baik, G. C. Kwon, J. J. Choi, G. S. Cho, H. S. Uhm, and E. H. Choi, *Plasma Chem. Plasma Process.* 34, 3 (2014).
20. K. Ninomiya, T. Ishijima, M. Imamura, T. Yamahara, H. Enomoto, K. Takahashi, Y. Tanaka, Y. Uesugi, and N. Shimizu, *J. Phys. D* 46, 42 (2013).
21. H. Duan, D. Wang, D. G. Kurth, and H. Möhwald, *Angew. Chem. Int. Ed.* 43, 42 (2004).
22. J. Li, X. Shao, Q. Zhou, M. Li, and Q. Zhang, *Appl. Surf. Sci.* 265 (2013).
23. S. Kango, S. Kalia, A. Celli, J. Njuguna, Y. Habibi, and R. Kumar, *Progress in Polymer Science* 38, 8 (2013).
24. B. Chen, Y. Gan, C. Zhu, J. Fei, Y. Jiang, L. Wang, X. Gao, X. He, W. Cai, and Z. Li, *IEEE Trans. Plasma Sci.* 44, 12 (2016).
25. Q. Wang, T. Shen, and S. Tong, *Ind. Eng. Chem. Res.* 55, 40 (2016).
26. P. Bruggeman and C. Leys, *J. Phys. D* 42, 5 (2009).
27. P. Bruggeman, F. Iza, D. Lauwers, and Y. A. Gonzalvo, *J. Phys. D* 43, 1 (2009).
28. P. Bruggeman, F. Iza, P. Guns, D. Lauwers, M. G. Kong, Y. A. Gonzalvo, C. Leys, and D. C. Schram, *Plasma Sources Sci. Technol.* 19, 1 (2009).
29. P. Bruggeman, G. Cunge, and N. Sadeghi, *Plasma Sources Sci. Technol.* 21, 3 (2012).
30. R. Hayashi, H. Obo, N. Takeuchi, and K. Yasuoka, *Electrical Engineering in Japan* 190, 3 (2015).
31. H. Uchiyama, Q. Zhao, M. A. Hassan, G. Andocs, N. Nojima, K. Takeda, K. Ishikawa, M. Hori, and T. Kondo, *PLoS One* 10, 8 (2015).
32. C. Liu, T. Kumakura, K. Ishikawa, H. Hashizume, K. Takeda, M. Ito, M. Hori, and J. Wu, *Plasma Sources Sci. Technol.* 25, 6 (2016).
33. Y. Matsuya, N. Takeuchi, and K. Yasuoka, *Electrical Engineering in Japan* 188, 2 (2014).
34. T. Verreycken, D. Schram, C. Leys, and P. Bruggeman, *Plasma Sources Sci. Technol.* 19, 4 (2010).
35. K. Yasuoka, K. Sasaki, R. Hayashi, A. Kosugi, and N. Takeuchi, *Int. J. Plasma Environ. Sci. Technol.* 4, 2 (2010).
36. N. Takeuchi, Y. Ishii, and K. Yasuoka, *Plasma Sources Sci. Technol.* 21, 1 (2012).
37. N. Takeuchi, Y. Kitagawa, A. Kosugi, K. Tachibana, H. Obo, and K. Yasuoka, *J. Phys. D* 47, 4 (2013).
38. M. R. Islam, M. Tushar, and H. Haniu, *J. Anal. Appl. Pyrolysis* 82, 1 (2008).
39. Y. Li, B. Han, L. Liu, F. Zhang, L. Zhang, S. Wen, Y. Lu, H. Yang, and J. Shen, *Composites Sci. Technol.* 88 (2013).
40. J. Barrand and J. Bokar, *SAE International Journal of Passenger Cars-Mechanical Systems* 1, 2008-01-0154 (2008).
41. L. Gonzalez, A. Rodriguez, J. De Benito, and A. Marcos, *Rubber Chem. Technol.* 69, 2 (1996).
42. G. Akovali and I. Ulkem, *Polymer* 40, 26 (1999).
43. M. Youssef, *Polym. Test.* 22, 2 (2003).
44. S. Jitkarnka, B. Chusaksri, P. Supaphol, and R. Magaraphan, *J. Anal. Appl. Pyrolysis* 80, 1 (2007).
45. W. H. Waddell and L. R. Evans, *Rubber Chem. Technol.* 69, 3 (1996).
46. G. Mathew, M. Huh, J. Rhee, M. Lee, and C. Nah, *Polym. Adv. Technol.* 15, 7 (2004).
47. G. Heideman, J. W. Noordermeer, and R. N. Datta, *B. van Baarle* 245, 1 (2006).
48. W. Kim, D. Lee, I. Kim, M. Son, W. Kim, and S. Cho, *Macromolecular Research* 17, 10 (2009).
49. L. Fulcheri and Y. Schwob, *Int. J. Hydrogen Energy* 20, 3 (1995).
50. J. Cho, H. Lee, and W. Yoo, *Int. J. Numer. Methods Eng.* 69, 7 (2007).
51. J. Cho, H. Lee, J. Sohn, G. Kim, and J. Woo, *European Journal of Mechanics-A/Solids* 25, 6 (2006).
52. X. Li, D. Banham, F. Feng, F. Forouzandeh, S. Ye, D. Y. Kwok, and V. Birss, *Carbon* 87 (2015).
53. H. Liu, S. Wang, Y. Xiao, and X. Li, *J. Mater. Sci.: Mater. Electron.* 27, 2 (2016).
54. M. K. Mun, J. W. Park, and G. Y. Yeom, *Plasma Processes and Polymers* 13, 7 (2016).
55. M. K. Mun, J. W. Park, J. H. Ahn, K. K. Kim, and G. Y. Yeom, *J. Nanosci. Nanotechnol.* 15, 10 (2015).
56. P. M. Hansson, P. M. Claesson, A. Swerin, W. H. Briscoe, J. Schoelkopf, P. A. Gane, and E. Thormann, *PCCP* 15, 41 (2013).
57. M. Li, W. Huang, and X. Wang, *Biointerphases* 10, 3 (2015).
58. E. Delzell, N. Sathiakumar, M. Hovinga, M. Macaluso, J. Julian, R. Larson, P. Cole, and D. C. Muir, *Toxicology* 113, 1 (1996).
59. A. F. Halasa, J. Prentis, B. Hsu, and C. Jasiunas, *Polymer* 46, 12 (2005).
60. H. Hsu, K. R. Leong, I. Teng, M. Halamiczek, J. Juang, S. Jian, L. Qian, and N. P. Kherani, *Materials* 7, 8 (2014).
61. E. P. Dillon, C. A. Crouse, and A. R. Barron, *Acs Nano* 2, 1 (2008).

Received: 5 December 2016. Accepted: 26 April 2017.